Excited State Dynamics initiated by an Electromagnetic Field within the Variational Multi-Configurational Gaussian (vMCG) method.

T.J. Penfold[a,*], M. Pápai[b], K.B. Møller[b], G.A. Worth[c,*]

[a]*Chemistry, School of Natural and Environmental Sciences, Newcastle University, Newcastle upon Tyne, NE1 7RU, United Kingdom.*
[b]*Department of Chemistry, Technical University of Denmark, DK-2800 Kongens Lyngby, Denmark.*
[c]*Department of Chemistry, University College London, 20, Gordon St., WC1H 0AJ London, United Kingdom.*

Abstract

The Variational Multi-Configurational Gaussian (vMCG) approach offers a framework to perform exact trajectory-based quantum dynamics, for which the quantum evolution of the Gaussian basis functions (GBFs) leads to a favourable convergence onto the solution of the time-dependent Schrödinger equation. For excited state dynamics seeking to interpret time-resolved pump-probe experiments, it is important to incorporate the effect of direct coupling to the external electromagnetic field to provide appropriate initial conditions for the ensuing dynamics. In this paper we use two model vibronic coupling Hamiltonians of pyrazine to explore, for the first time, the influence of the coupling between the external field and the GBFs in vMCG on the dynamics. We show that when the excitation pulse is short compared to the nuclear dynamics, vertical projection without a field and explicit description of the external field converge on the same dynamics. However, for longer pulses, a sizeable change in the population dynamics is observed. We demonstrate that comparatively few GBF are sufficient to provide qualitative agreement to full MCTDH dynamics and a quantitative agreement can often be achieved using ~100 GBFs. Longer pulses require more GBFs due to the prolonged coupling between the ground and excited states. Finally, even for dynamics when the majority of the population remains in the harmonic ground state, the single set formalism offers the fastest convergence.

Keywords: variational multi-configurational Gaussian method, Quantum Dynamics, Nonadiabatic, external field

1. Introduction

The rapid development in laser technology has enabled the implementation of a wide range of spectroscopic techniques which facilitate the measurement, and even control, of matter by light with an increased level of detail [1, 2, 3]. In particular, ultrafast pump-probe experiments used to understand excited state processes are increasingly common. From a theoretical perspective, an accurate description of molecular dynamics in excited electronic states, when the Born-Oppenheimer approximation may break down, is required for understanding light-triggered phenomena. However, an important, yet often overlooked aspect when seeking a synergy between experiment and theory is that the latter should include the description of the external field which generates the initial photoexcited state [4].

Quantum dynamics simulations including the explicit description of an external field are well established [5], and have been extended to propose shaped later pulses to control the outcome of reactions [6]. In addition to traditional grid-based methods, trajectory based methods [7, 8, 9] including explicit light-matter

interactions are becoming increasingly common. These are more amenable to direct-dynamics implementations, whereby the potential and couplings are calculated *on-the-fly*, and are thus more suitable for the complete description of large amplitude motions.

For excited state processes, the focus of the present work, one of the most popular methods, which moves in this direction is Tully's Trajectory Surface Hopping (TSH) [10, 11], widely adopted due to its computational efficiency. Here the nuclear wavepacket is represented by a swarm of classically evolving independent point (delta functions) trajectories, and therefore while computationally efficient and accurate in a number of cases, this approach can offer no guarantee that the calculations converge onto the quantum mechanical solution. Multiple previous studies have coupled such dynamics with external fields and found good agreement for model systems, usually in one- or two- nuclear degrees of freedom [12, 13, 14, 15, 16, 17], although the effect of the independent trajectory approximation has to be considered [18, 19].

An alternative approach for a trajectory based dynamics, which retains a quantum description uses Gaussian basis functions. This motivation originates from the work of Heller [20, 21, 22] who adopted an expansion of the nuclear wavefunction in terms of a moving Gaussian basis set. A number of methods exploiting a Gaussian basis set representation have been developed. These include multiple spawning [23, 24], coupled-coherent states (CCS) [25], multi-configurational Ehrenfest (MCE) [26] and the multiple cloning method [27]. Recently, Mignolet *et al.* have extended the framework of Multiple Spawning to incorporate the effect of both atto- and femtosecond laser pulses [28, 29]. This was benchmarked against numerically exact quantum dynamics simulations for a model for LiH and the effect of nuclear motion on the photoexcitation of a sulfine (H_2CSO), showing good agreement for initial conditions including 100 uncoupled initial conditions sampled from a Wigner distribution.

In each of the aforementioned Gaussian basis set approaches, the equations of motion governing the evolution of the GBF (position and momentum) are solved within the Newtonian limit. The ability to achieve the exact quantum description of the dynamics is not affected by the choice of how the GBF are evolved. However, the choice of equations of motion for the basis functions does substantially influence the rate at which this limit is reached. Indeed, classical (uncorrelated) motion of the basis set tends to limit phase space covered by the trajectories, although with judicious choice of initial conditions rapid convergence can still be achieved. To overcome this, an alternative approach is to adopt the fully quantum variational solution, in which the basis functions move along quantum trajectories. One approach that achieves this is variational multi-configurational Gaussian (vMCG) method [7] , which can be considered as the GBF equivalent of the Multi Configurational Time-dependent Hartree (MCTDH) method [30, 31].

The use of quantum trajectories means that compared to the other GBF approaches, vMCG converges to the exact solution to the molecular time-dependent Schrödinger equation with a smaller basis set. In their original work, Worth and co-workers [32] demonstrated the method by comparing vMCG with MCTDH dynamics using a model Hamiltonian of the Butatriene cation containing five nuclear and two electronic degrees of freedom. Despite a small basis set composed of 16 GBF for each state, vMCG gave good agreement, for time <30 fs) to the MCTDH dynamics, while similar agreement for the model Hamiltonian of pyrazine [33] has also been achieved [7].

In this paper we use two model vibronic coupling Hamiltonians of pyrazine [33, 34] to explore the effect of the external field on the photoexcitation process. Using direct projection of the ground state wavefunction, interactions with 10 fs, 60 fs and 150 fs laser pulses, we show that the qualitative agreement between vMCG and MCTDH can be achieved using relatively few GBFs, and is much faster than the classical counterpart (clMCG). The convergence towards a quantitative agreement requires ∼100 GBF, but is affected by the dimensionality of the model Hamiltonian and the length of the external field. Throughout the single set formalism remains the most efficient way to perform the simulations.

2. Theory and Computational Details

2.1. Variational Multi-configurational Gaussian (vMCG)

For details of the vMCG method, readers are referred to refs [35, 36, 37, 7, 38]. Briefly, the derivation of the vMCG method begins by representing the molecular wavefunction, $\Psi(\boldsymbol{r}, \boldsymbol{R}, t)$, as the product of the
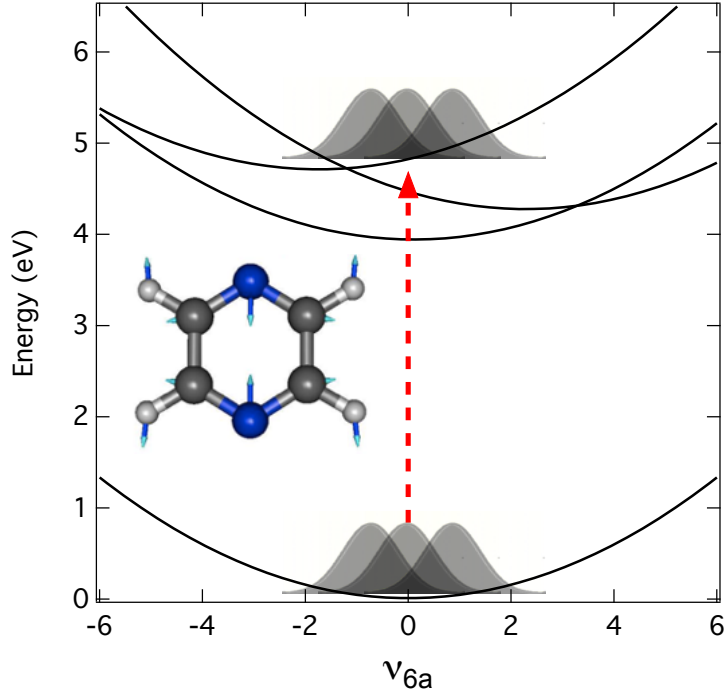
Figure 1: Potential energy curves of the ground and lowest 3 excited states ($B_{3u}(n\pi^*)$, $A_u(n\pi^*)$ and $B_{2u}(\pi\pi^*)$) of pyrazine along ν_{6a} (shown inset left). The excited states is generated by either vertical projection or by direct interaction with an external electromagnetic field.

electronic wavefunction ($\psi^{(s)}(\mathbf{r})$), $\chi_j^{(s)}(\mathbf{R}, t)$ is a swarm of j GBF, weighted by time-dependent coefficients ($A_j^{(s)}$):

$$\Psi(\mathbf{r}, \mathbf{R}, t) = \sum_s \sum_j A_j^{(s)}(t) \psi^{(s)}(\mathbf{r}) \chi_j^{(s)}(\mathbf{R}, t) \tag{1}$$

This *ansatz* contains, as illustrated by the sum over s electronic states, a set of GBFs for each state. This is the multi-set formalism. In contrast, for the single set formalism, the s superscript is dropped from all future equations and the *ansatz* becomes:

$$\Psi(\mathbf{r}, \mathbf{R}, t) = \sum_j A_j(t) \psi(\mathbf{r}) \chi_j(\mathbf{R}, t) \tag{2}$$

In this single-set formalism each basis trajectory has a time-dependent expansion coefficient for every electronic states. The GBFs in the single-set formalism evolve under a state-averaged mean field and therefore this is usually considered to be an advantageous treatment if the dynamics in the different electronic states is similar, e.g., when the surfaces are almost parallel. Within the MCTDH framework, the multi-set formalism is more commonly most efficient as dynamics on various diabatic states can be rather different. However, previous work [7] has shown that within vMCG the single-set formalism remains preferred. This is discussed in more detail below.

The GBF can be expressed:

$$\chi_j(\mathbf{R}, t) = \prod_\alpha (2\pi\sigma_\alpha^2)^{-1/4} \exp\left(-\frac{1}{4\sigma_\alpha^2}[R_\alpha - R_{j\alpha}(t)]^2 + i\frac{p_{j\alpha}(t)}{\hbar}R_\alpha + i\gamma\right) \tag{3}$$

where $\mathbf{R}$ and $\mathbf{p}$ are the position and momentum of the GBFs along each degree of freedom, α. σ is the wavepacket width and γ is the phase term which carries the quantum information. In the interest of numerical stability, σ is kept fixed. The nuclear wavefunction is therefore a superposition of frozen GBFs [21].

The vMCG equations of motion (EOM), derived using the Dirac-Frenkel variational principle [39, 40] are:

$$i\sum_l \dot{A}_l = S_{jl}^{-1}\sum_l (H_{jl} - i\tau_{jl})A_l \tag{4}$$

and:

$$i\dot{\Lambda} = C^{-1}Y \tag{5}$$

for the evolution of the GBFs where

$$C_{j\alpha,l\beta} = \rho_{jl}\left(\sum_\beta S_{jl}^{\alpha\beta} - [S^{(\alpha 0)} \cdot S^{-1} \cdot S^{0\beta}]_{jl}\right) \tag{6}$$

and

$$Y_{j\alpha} = \sum_l \rho_{jl}\left(H_{jl} - [S^{(\alpha 0)} \cdot S^{-1} \cdot H]_{jl}\right) \tag{7}$$

where H_{jl} are elements of the Hamiltonian matrix, S_{jl} and τ_{jl} are elements of the overlap matrix and time-derivative matrix, respectively. The interaction terms added to the Hamiltonian, described in the following section, enter the EOMs through H_{jl}. It is noted that the EOM for the time-dependent coefficients are the same as the one for the multiple spawning method [23] and only differs from the standard MCTDH expansion coefficient EOMs by the requirement to address, using S^{-1}, the non-orthogonality of the GBFs.

In the context of the future discussions within the paper and drawing the connections between the vMCG and other GBF approaches, Equation 6 can separate the propagation of the Gaussian parameters into uncorrelated (classical) and correlated (quantum) terms [37]. Indeed, besides the time-dependence of the basis set size of the multiple spawning algorithm, it is the inclusion of the quantum correction on the nuclear motion which captures all the key differences between vMCG and multiple spawning. This is to say that in the former the GBF are correlated and follow quantum trajectories, while in the latter they are uncorrelated and therefore follows classical motion. This division is achieved using a power series expansion in terms of Gaussian moments leading to:

$$i\dot{\Lambda} = X_0 + C^{-1}Y_R \tag{8}$$

The first term, X_0 contains the terms responsible for the separable classical motion of the GBF, while $C^{-1}Y_R$ contains all of the non-classical parts of the nuclear dynamics. Analysis of Y_R shows that the correlation between the GBF depend mostly on the second derivatives of the potential at the centre of the GBFs, and so the GBFs are coupled due to the differing curvature of the potential experienced by each function. In this work, truncating the EOM's to only X_0 is denoted as clMCG [37].

2.2. Model Hamiltonian and Time-dependent Interaction

The simulations have been performed using 2 model vibronic coupling Hamiltonians (See Table 1). The first, based upon the established model for pyrazine [41] includes 5 normal modes (ν_{6a}, ν_{10a}, ν_1, ν_{8a}, ν_{9a}), the electronic ground state and two excited, $\text{B}_{2u}(\pi\pi^*)$ and $\text{B}_{3u}(n\pi^*)$, states. The second was recently proposed by Lasorne et al. [34]. In contrast to the more commonly used model [41] which incorporates the role of the strong non-adiabatic effects due to the existence of a conical intersection between the $\text{B}_{2u}(\pi\pi^*)$ and $\text{B}_{3u}(n\pi^*)$ electronic states, this model Hamiltonian also includes the $\text{A}_u(n\pi^*)$ state [34]. In this model 9 modes were included, these are ν_1, ν_3, ν_4, ν_5, ν_{6a}, ν_{8a}, ν_{8b}, ν_{9a} ν_{10a}.

In both models, the Hamiltonian (H_{vib}) is supplemented by the interaction with the external field:

$$\hat{H} = H_{vib} + H_{int} \tag{9}$$

4

The coupling to the external field ($\hat{H}_{int}$) is assumed to be a dipole interaction:

$$H_{int} = -\mu_{IJ} \cdot \mathbf{E}(t) \tag{10}$$

where μ is the transition dipole and $\mathbf{E}$ the electric field of the pulse. In the present work we take the transition dipole moment between the ground state and the optically bright state, $B_{2u}(\pi\pi^*)$ to be 0.1. The pulses has a Gaussian shape with a variable full-width half maximum as described in the results. The central frequency is 4.8 eV, i.e. resonant with the optically bright $B_{2u}(\pi\pi^*)$ state.

2.3. Computational Details

All simulations have been performed using vMCG or clMCG as implemented within a development version of the Quantics quantum dynamics package [30, 31]. In all simulations the full integrals to 4th order were calculated so that convergence to the full quantum dynamics result is guaranteed. Propagation was performed using frozen-width GBFs. In all cases, the initial ground state wavefunction was composed of a Gaussian function with amplitude 1.0 centred at the Franck-Condon geometry surrounded by additional basis functions with amplitude 0 and an overlap of 0.6. All basis functions had a fixed width, $\langle dQ \rangle = 0.7$. For the vMCG simulations, to assist with issues related to singularities and the C-matrix inversion we have used the Tikhonov regularisation and the dynamical coupling approach [42]. Consistent with previous observations [7], the single-set representation leads to faster convergence, even in the presence of the field and therefore this representation is used throughout. The benchmark MCTDH simulations were performed using the multi-set formalism and the details are shown in Table 1.

5 mode 3 state	Combination of Modes	Number of SPFs	Number of Grid Points
Without Pulse	(ν_{6a}, ν_{10a}), $(\nu_1, \nu_{8a}, \nu_{9a})$	(2,40,40), (2,40,40)	(35,35), (35,35)
With Pulse	(ν_{6a}, ν_{10a}), $(\nu_1, \nu_{8a}, \nu_{9a})$	(2,40,40), (2,40,40)	(35,35), (35,35)

9 mode 4 state	Combination of Modes	Number of SPFs	Number of Grid Points
Without Pulse	(ν_{6a}, ν_{10a}), (ν_1, ν_4),	(1,40,40,40), (1,40,40,40)	(35,35), (35,35)
	$(\nu_3, \nu_{9a}, \nu_{8b})$, (ν_5, ν_{8a})	(1,40,40,40), (1,30,30,30)	(15,15,15), (35,35)
With Pulse	(ν_{6a}, ν_{10a}), (ν_1, ν_4),	(10,40,40,40), (10,40,40,40)	(35,35), (35,35)
	$(\nu_3, \nu_{9a}, \nu_{8b})$, (ν_5, ν_{8a})	(10,40,40,40), (10,30,30,30)	(15,15,15), (35,35)

Table 1: Details of the MCTDH calculations performed for the two model Hamiltonians including the mode combination, number of single particle functions (SPFs) and primitive basis functions used.

3. Results

3.1. Excited State Non-adiabatic Dynamics via Vertical Projection

Figure 2 shows the excited state population kinetics using the 9 mode 4 state model after vertical projection of the ground state wavefunction into the bright $B_{2u}(\pi\pi^*)$ excited state at the Franck-Condon geometry. In agreement with the results in ref. [34], the dynamics performed with MCTDH (solid lines) exhibit a rapid decay of the initially excited $B_{2u}(\pi\pi^*)$ state into the both the $B_{3u}(n\pi^*)$ and $A_u(n\pi^*)$ states. Both states rise simultaneously, but it is the lower $B_{3u}(n\pi^*)$ which dominates at 500 fs. The population kinetics exhibit clear oscillations, which are in phase for the $B_{3u}(n\pi^*)$ and $A_u(n\pi^*)$ states, but out of phase for $B_{2u}(\pi\pi^*)$. These have a period of $\sim$65 fs (513 cm^{-1}), which is in close agreement with the frequency of the ν_{6a} mode (Figure 1) along which the main population transfer occurs.

The dashed lines in Figures 2a and b correspond to the same simulations performed with vMCG using 25 and 100 GBFs, respectively. While neither completely converge onto the MCTDH solution, even using only 25 GBF, there is qualitative agreement with between the population kinetics observed in both cases over the entire 500 fs of the simulations. The main difference is that the 100 GBF improves the description of the 65
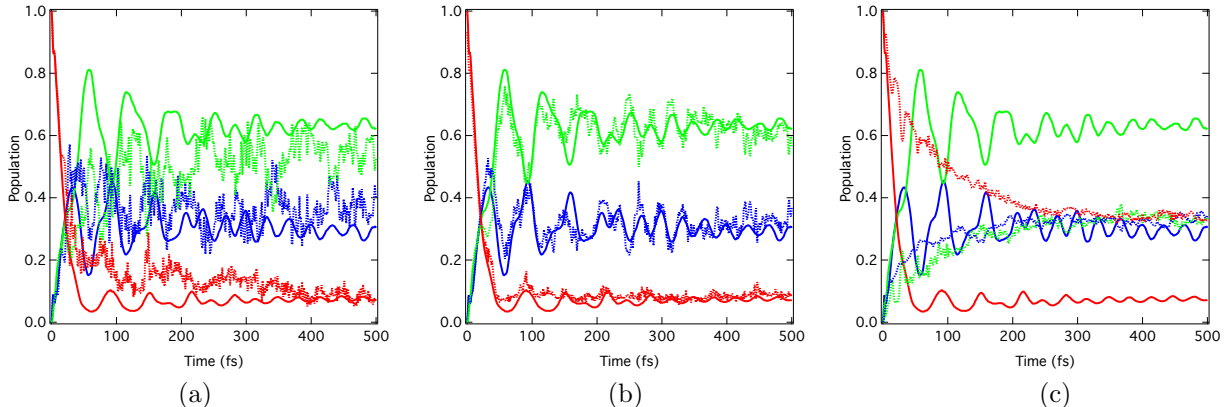
Figure 2: Electronic state diabatic populations of the $B_{3u}(n\pi^*$,green), $A_u(n\pi^*$,blue) and $B_{2u}(\pi\pi^*$, red) states (dashed lines) computed using (a) 25 vMCG GBFs, (b) 100 vMCG GBFs and (c) 200 clMCG GBFs compared to MCTDH simulations (solid lines) performed for the 9 mode 4 state model. In this case the initially excited state is generated by projection of the GBFs in the ground state into the $B_{2u}(\pi\pi^*)$ state.

fs coherent oscillations. This is consistent with previous similar observation for the 4-mode 2 state model of pyrazine [7], although the larger model used in the present study requires more GBFs, 100 compared to 60 used in ref. [7]. Throughout these simulations, the single-set formalism provided the quickest convergence. While the multi-set formalism enables the basis functions on each state to adapt to its state, it still requires more basis functions overall leading to a slower convergence.

Figure 2c shows the populations kinetics for clMCG using 200 GBF. This clearly exhibits incorrect dynamics and many more GBF would be required to reach convergence. However, despite the simpler equations of motion and increased numerical stability of clMCG, this simulation is a similar time (28 hrs) to vMCG using 100 GBF shown in Figure 2b. Interestingly, the vMCG simulations using 25 GBFs, which captures the main essence of the dynamics, takes just over 2 hrs. All of these compare favourably to the MCTDH dynamics which takes 20 hrs. All time quoted correspond to simulations performed using a single thread of an Intel Xeon Processor E5-2620v4 2.10 GHz.

3.2. Excited State Non-adiabatic Dynamics Initiated by Laser Excitation

We now turn our attention to the excited state dynamics using the 9 mode 4 state model, initiated by direct interaction with an external electromagnetic field. Figure 3 shows the excited state diabatic populations (a,c,e) and the absolute value of the autocorrelation function (b,d,f) for the dynamics initiated by a 10 fs pulse. The MCTDH population dynamics (solid lines) are very similar to the direct projection of the wavepacket (Figure 2) as one would expect for such a short excitation as the nuclear wavepacket does not have time to move significantly during the excitation.

The vMCG dynamics with 25 (a) and 100 (b) vMCG GBFs and 200 clMCG (c) GBFs also exhibit similar population kinetics compared to those observed in Figure 2. The convergence of both vMCG simulations is slightly worse than its corresponding dynamics without the laser pulse. This difference originates from the period when the pulse is present, i.e. the additional coupling between ground and excited states. This additional step of transfer of population from the ground to the excited state requires a slightly more converged description of the wavefunction in the ground and excited states and therefore more GBFs. For the 10 fs pulse, it is also possible to small excited state populations contribute to this slightly. The absolute value of the autocorrelation function (Figure 3b,d and f) exhibits similar trends in comparison to the population kinetics. Indeed, for the clGWP trajectories, the correct structure, especially for ≤100 fs is broadly observed. However, at later times in comparison to the autocorrelation function obtained using vMCG the oscillations in this overlap is too strong. This is because the uncoupled GBF occupy a smaller
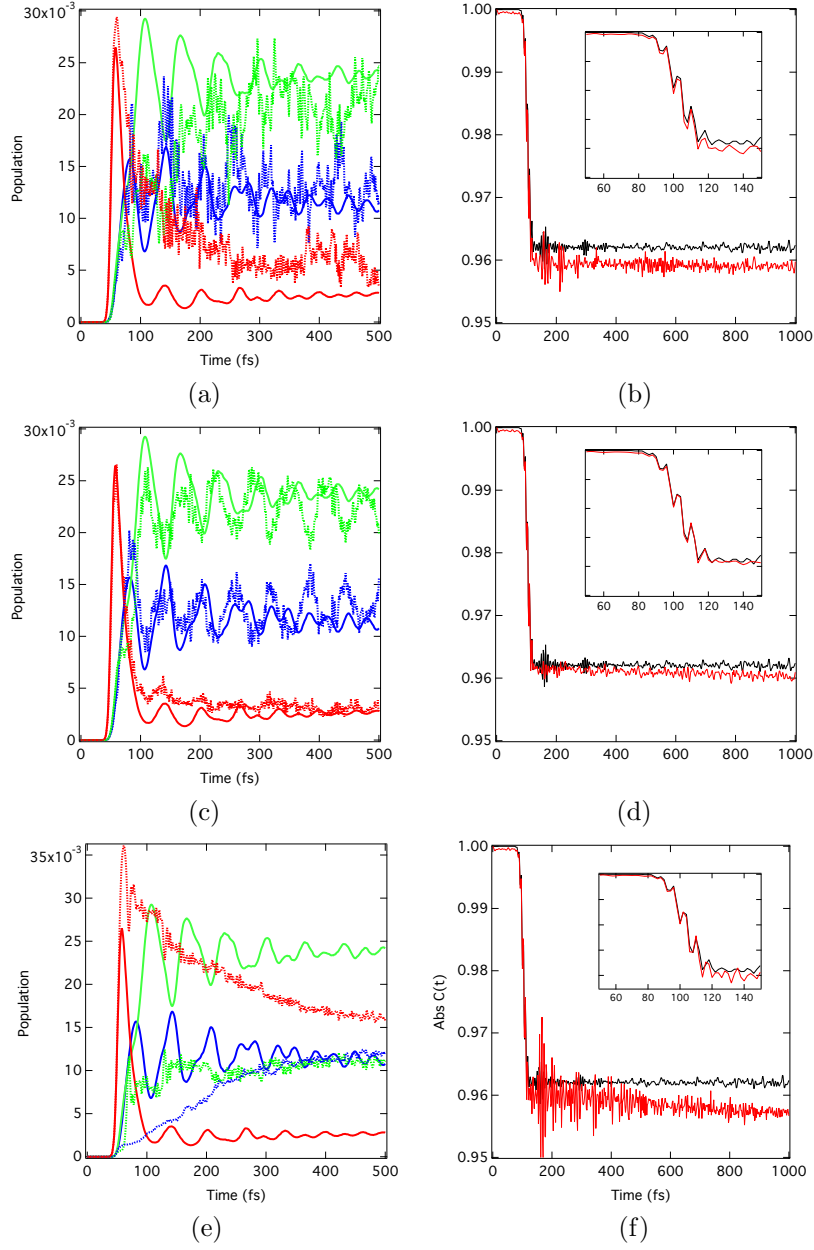
Figure 3: Electronic state diabatic populations (a,c,e) of the $B_{3u}(n\pi^*$,green), $A_u(n\pi^*$,blue) and $B_{2u}(\pi\pi^*$, red) states (dashed lines) and the absolute value of the autocorrelation function (b,d,f) computed using (a,b) 25 vMCG GBFs, (c,d) 100 vMCG GBFs and (e,f) 200 clMCG GBFs compared to MCTDH simulations (solid lines) performed for the 9 mode 4 state model. In this case the excited state is 10 fs laser pulse as described in the methods section.
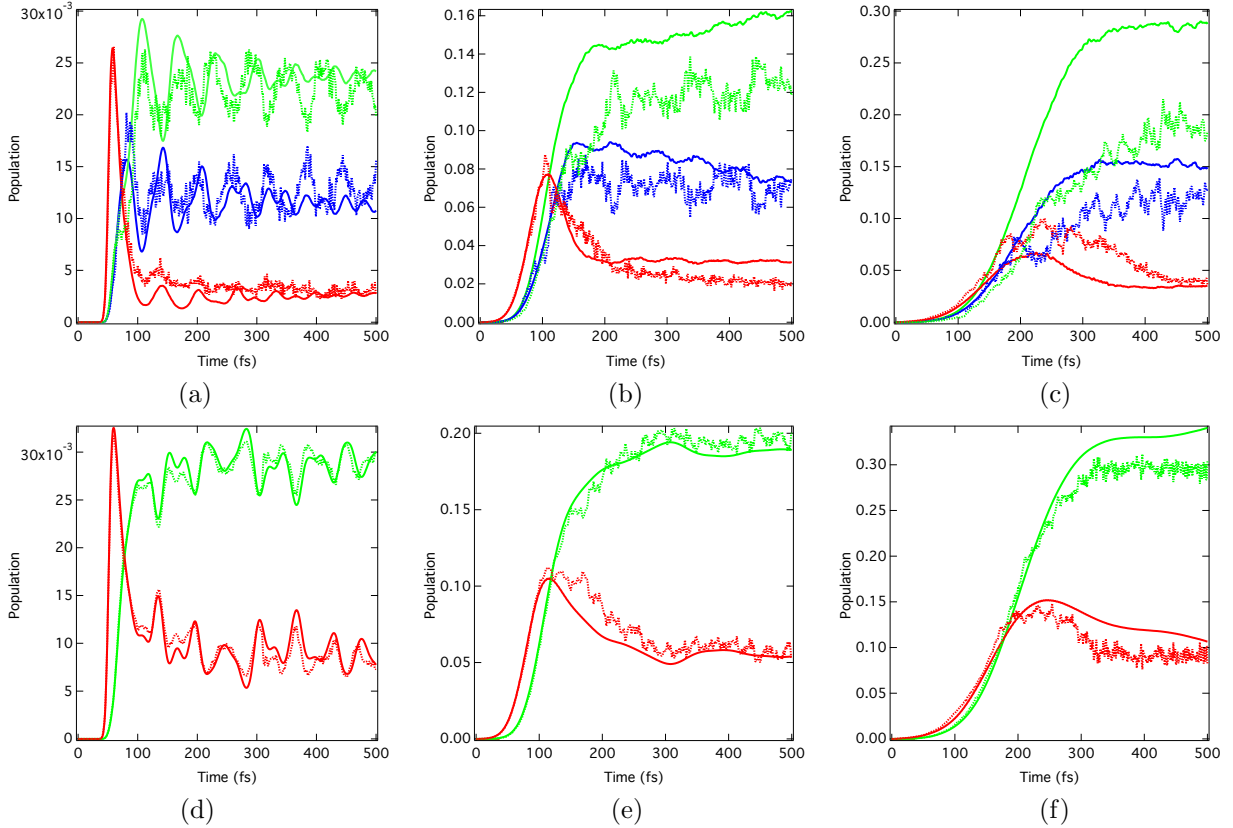
7

Figure 4: Electronic state diabatic populations of the $B_{3u}(n\pi^*$,green), $A_u(n\pi^*$,blue) and $B_{2u}(\pi\pi^*$, red) states (dashed lines) computed using 100 vMCG GBFs compared to MCTDH simulations (solid lines) performed for the 9 mode 4 state model. In this case the initially excited state is generated by interaction of the GBFs in the ground state with an external electromagnetic field with full-width half maximum of (a) 10 fs, (b) 60 fs and (c) 150 fs. The corresponding simulations using the 5 mode 3 state model are shown in (d) 10 fs, (e) 60 fs and (f) 150 fs with the same colouring labelling for the states. The $B_{3u}(n\pi^*)$ state is green and the $B_{2u}(\pi\pi^*)$ state is red.

region of phase space, therefore movement will have a stronger effect on correlation function and therefore clearly many more functions will be needed for a converged result.

Importantly, these simulations illustrate that even when the majority of the population remains in the Harmonic ground state, which is both far from parallel with respect to the excited state potentials and exhibits little motion away from the Franck-Condon geometry, the singlet-set formalism remains favourable and incorporating the ability for the excited state GBF to adapt independently is not required.

Figure 4 shows the population kinetics for three vMCG simulations all using 100 GBFs and the 9 mode 4 state model but with pulses of 10 fs (a), 60 fs (b) and 150 fs (c). The corresponding simulations using the 5 mode 3 state model are shown in Figure 4d,e and f for 10, 60 and 150 fs pulses, respectively. The first notable difference between the simulations shown in Figures 4a-c, is the loss of the wavepacket dynamics for the longer pulses. They remain weakly visible for the 60 fs pulse, but when the length of the pulse exceeds the period of the oscillations they are no longer visible. The populations kinetics also illustrates that convergence is reduced for the excitations for the longer pulses. This is most clearly visible during the 150 fs pulse for which the population dynamics is far from quantitative. The origin for the loss of agreement for 100 GBF is because, as observed in Figure 3, the agreement of the absolute autocorrelation function between the vMCG and MCTDH simulations is lost at longer times. This does not represent a problem for the shorter pulses, as the coupling between the ground and excited state, i.e. the external field, is only

present while the structure of the autocorrelation function is in good agreement. However, for the longer time simulations the coupling is still present while the phase and amplitude of the vMCG and MCTDH autocorrelation functions offer less agreement, giving rise to the error in the simulations.

Figures 4d-f show the corresponding dynamics for the 5 mode 3 state model. The absence of the $A_u(n\pi^*)$ in this case means that population transfer only occurs between the $B_{2u}(\pi\pi^*$, red) and $B_{3u}(n\pi^*$,green) states. A similar trend is observed, with convergence for 100 GBFs decreasing as a function of the pulse length, however the reduced dimensionality of the model Hamiltonian makes achieving convergence easier and even for the 150 fs, quantitative agreement between the MCTDH and vMCG simulations is observed.

4. Discussion and Conclusions

Pump-probe techniques applying short (fs-ps) pulses have played a key role in resolving excited-state dynamics. To achieve an effective synergy, it is important that simulations replicate the important experimental conditions. This includes the interaction between the molecule and the external time-dependent electric field of the laser pulse that generates the electronically excited state. However, the most common approach for initiating excited-state dynamics is the instantaneous projection of the nuclear wave function from the electronic ground state onto the excited-state potential energy surface. This approach assumes that the excitation is impulsive in that no nuclear dynamics can occur during excitation and that the pump pulse prepares a well-defined excited state. In the present contribution we seek to facilitate an accurate framework for Gaussian based quantum dynamics to simulate time-resolved spectra [43, 44, 45, 46]. We have used two model vibronic coupling Hamiltonians for pyrazine to explore the influence of the coupling between the external field and the GBFs within the framework of vMCG dynamics.

We have shown that the most commonly adopted approach of vertical projection of the wavepacket provides a good correspondence to dynamics excited using very short pulses (10 fs) as the excitation processes is faster than any nuclear motion in the system and therefore it can be assumed to be impulsive. In addition, this spectrally broad pulse facilitates the generation of the coherent nuclear wavepacket, which is absent for the pulses of $\geq$60 fs. Our present results show that even for comparatively few GBFs (25 or 100), agreement between MCTDH dynamics and vMCG is observed, at reduced or comparable computational cost. As the length of the external field is increased, more GBFs are required to retain the agreement between the vMCG and MCTDH. The external field, alongside the dimensionality of the Hamiltonian does therefore represent an additional challenging for converging GBF quantum dynamics. Throughout this work, the singlet set formalism was found to provide the most rapid convergence.

Finally, it is noted that in agreement with dynamics without external electromagnetic fields, vMCG exhibits significantly enhanced superior convergence to clMCG dynamics. However, it is important to note that in both cases the initial conditions were the same. In contrast to other GBF methods, vMCG is insensitive to the choice of initial basis functions, as the variational nature means that the basis functions will follow the evolving wavepacket as well as possible and the same result is obtained irrespective of where they all start. In addition, the present simulations only involve bound states and relatively small vibrational amplitudes which may also favour vMCG. Further work should consider extending these simulations to larger amplitude motions to see if the trend observed in the present work remains the same.

5. Acknowledgements

References

[1] Lin X Chen, X Zhang, and ML Shelby. Recent advances on ultrafast x-ray spectroscopy in the chemical sciences. *Chemical Science*, 5(11):4136–4152, 2014.

[2] Majed Chergui and Ahmed H Zewail. Electron and x-ray methods of ultrafast structural dynamics: Advances and applications. *ChemPhysChem*, 10(1):28–43, 2009.

[3] Thomas AA Oliver. Recent advances in multidimensional ultrafast spectroscopy. *Royal Society open science*, 5(1):171425, 2018.

[4] Jiří Suchan, Daniel Hollas, Basile FE Curchod, and Petr Slavíček. On the importance of initial conditions for excited-state dynamics. *Faraday discussions*, 212:307–330, 2018.

[5] Mátyás Pápai, Mats Simmermacher, Thomas J Penfold, Klaus B Møller, and Tamas Rozgonyi. How to excite nuclear wavepackets into electronically degenerate states in spin-vibronic quantum dynamics simulations. *Journal of Chemical Theory and Computation*, 14(8):3967–3974, 2018.

[6] T J Penfold, GA Worth, and C Meier. Local control of multidimensional dynamics. *Physical Chemistry Chemical Physics*, 12(48):15616–15627, 2010.

[7] G W Richings, I Polyak, K E Spinlove, GA Worth, I Burghardt, and B Lasorne. Quantum dynamics simulations using Gaussian wavepackets: the vMCG method. *International Reviews In Physical Chemistry*, 34(2):269–308, July 2015.

[8] Rachel Crespo-Otero and Mario Barbatti. Recent advances and perspectives on nonadiabatic mixed quantum–classical dynamics. *Chemical reviews*, 118(15):7026–7068, 2018.

[9] Basile FE Curchod and Todd J Martínez. Ab initio nonadiabatic quantum molecular dynamics. *Chemical reviews*, 118(7):3305–3336, 2018.

[10] John C. Tully and Richard K. Preston. Trajectory Surface Hopping Approach to Nonadiabatic Molecular Collisions: The Reaction of H+ with D2. *The Journal of Chemical Physics*, 55(2):562–572, July 1971.

[11] J. C. Tully. Molecular dynamics with electronic transitions. *Journal of Chemical Physics*, 93:1061–1071, 1990.

[12] Roland Mitrić, Jens Petersen, and Vlasta Bonačić-Kouteckỳ. Laser-field-induced surface-hopping method for the simulation and control of ultrafast photodynamics. *Physical Review A*, 79(5):053416, 2009.

[13] Martin Richter, Philipp Marquetand, Jesús González-Vázquez, Ignacio Sola, and Leticia González. Sharc: ab initio molecular dynamics with surface hopping in the adiabatic representation including arbitrary couplings. *Journal of chemical theory and computation*, 7(5):1253–1258, 2011.

[14] Philipp Marquetand, Martin Richter, Jesús González-Vázquez, Ignacio Sola, and Leticia González. Nonadiabatic ab initio molecular dynamics including spin–orbit coupling and laser fields. *Faraday discussions*, 153:261–273, 2011.

[15] I. Tavernelli, B. F. E. Curchod, and U. Rothlisberger. Mixed quantum-classical dynamics with time-dependent external fields: A time-dependent density-functional-theory approach. *Phys. Rev. A*, 81:052508, 2010.

[16] Roland Mitric, Jens Petersen, Matthias Wohlgemuth, Ute Werner, Vlasta Bonacic-Koutecky, Ludger Woste, and Joshua Jortner. Time-resolved femtosecond photoelectron spectroscopy by field-induced surface hopping. *The Journal of Physical Chemistry A*, 115(16):3755–3765, 2010.

[17] Basile FE Curchod, Thomas J Penfold, Ursula Rothlisberger, and Ivano Tavernelli. Local control theory in trajectory surface hopping dynamics applied to the excited-state proton transfer of 4-hydroxyacridine. *ChemPhysChem*, 16(10):2127–2133, 2015.

[18] B F E Curchod, T J Penfold, U Rothlisberger, and I Tavernelli. Local control theory in trajectory-based nonadiabatic dynamics. *Physical Review A*, 84:042507, 2011.

[19] Benoit Mignolet and Basile FE Curchod. Excited-state molecular dynamics triggered by light pulses–ab initio multiple spawning vs trajectory surface hopping. *The Journal of Physical Chemistry A*, 2019.

[20] Eric J Heller. Time-dependent approach to semiclassical dynamics. *The Journal of Chemical Physics*, 62(4):1544–1555, 1975.

[21] Eric J Heller. Frozen gaussians: A very simple semiclassical approximation. *The Journal of Chemical Physics*, 75(6):2923–2931, 1981.

[22] Soo-Y Lee and Eric J Heller. Exact time-dependent wave packet propagation: Application to the photodissociation of methyl iodide. *The Journal of Chemical Physics*, 76(6):3035–3044, 1982.

[23] Todd J Martinez, M Ben-Nun, and RD Levine. Multi-electronic-state molecular dynamics: A wave function approach with applications. *The Journal of Physical Chemistry*, 100(19):7884–7895, 1996.

[24] M Ben-Nun and Todd J Martınez. Nonadiabatic molecular dynamics: Validation of the multiple spawning method for a multidimensional problem. *The Journal of chemical physics*, 108(17):7244–7257, 1998.

[25] Dmitrii V Shalashilin and Mark S Child. The phase space ccs approach to quantum and semiclassical molecular dynamics for high-dimensional systems. *Chemical physics*, 304(1):103–120, 2004.

[26] Dmitrii V Shalashilin. Quantum mechanics with the basis set guided by ehrenfest trajectories: Theory and application to spin-boson model. *The Journal of chemical physics*, 130(24):244101, 2009.

[27] Dmitry V Makhov, William J Glover, Todd J Martinez, and Dmitrii V Shalashilin. Ab initio multiple cloning algorithm for quantum nonadiabatic molecular dynamics. *The Journal of chemical physics*, 141(5):054110, 2014.

[28] Benoit Mignolet, Basile FE Curchod, and Todd J Martínez. Communication: Xfaimsexternal field ab initio multiple spawning for electron-nuclear dynamics triggered by short laser pulses. *The Journal of chemical physics*, 145(19):191104, 2016.

[29] Benoit Mignolet and Basile FE Curchod. A walk through the approximations of ab initio multiple spawning. *The Journal of chemical physics*, 148(13):134110, 2018.

[30] M. H. Beck, A. Jäckle, G. A. Worth, and H.-D. Meyer. The multiconfiguration time-dependent Hartree method: A highly efficient algorithm for propagating wavepackets. *Phys. Rep.*, 324:1–105, 2000.

[31] H.-D. Meyer, F. Gatti, and G. A. Worth, editors. *High dimensional quantum dynamics: Basic Theory, Extensions, and Applications of the MCTDH method*. VCH, Weinheim, Germany, 2008.

[32] GA Worth, MA Robb, and I Burghardt. A novel algorithm for non-adiabatic direct dynamics using variational gaussian wavepackets. *Faraday discussions*, 127:307–323, 2004.

[33] A Raab, GA Worth, H-D Meyer, and LS Cederbaum. Molecular dynamics of pyrazine after excitation to the s 2 electronic

state using a realistic 24-mode model hamiltonian. *The Journal of chemical physics*, 110(2):936–946, 1999.

[34] Matthieu Sala, Benjamin Lasorne, Fabien Gatti, and Stéphane Guérin. The role of the low-lying dark nπ* states in the photophysics of pyrazine: a quantum dynamics study. *Physical Chemistry Chemical Physics*, 16(30):15957–15967, 2014.

[35] I Burghardt, H-D Meyer, and LS Cederbaum. Approaches to the approximate treatment of complex molecular systems by the multiconfiguration time-dependent hartree method. *The Journal of chemical physics*, 111(7):2927–2939, 1999.

[36] GA Worth, MA Robb, and I Burghardt. A novel algorithm for non-adiabatic direct dynamics using variational Gaussian wavepackets. *Faraday Discussions*, 127:307–323, 2004.

[37] I Burghardt, K Giri, and GA Worth. Multimode quantum dynamics using gaussian wavepackets: The gaussian-based multiconfiguration time-dependent hartree (g-mctdh) method applied to the absorption spectrum of pyrazine. *The Journal of chemical physics*, 129(17):174104, 2008.

[38] Morgane Vacher, Michael J Bearpark, and Michael A Robb. Direct methods for non-adiabatic dynamics: connecting the single-set variational multi-configuration gaussian (vmcg) and ehrenfest perspectives. *Theoretical Chemistry Accounts*, 135(8):1–11, 2016.

[39] Paul AM Dirac. Note on exchange phenomena in the thomas atom. In *Mathematical Proceedings of the Cambridge Philosophical Society*, volume 26, pages 376–385. Cambridge Univ Press, 1930.

[40] Iakov Ilich Frenkel, Jakov Ilič Frenkel, Jakov Ilič Frenkel, Russia Physicist, Jakov Ilič Frenkel, and Russie Physicien. *Wave mechanics: advanced general theory*. Clarendon Press Oxford, 1934.

[41] A Raab, GA Worth, H-D Meyer, and LS Cederbaum. Molecular dynamics of pyrazine after excitation to the S[sub 2] electronic state using a realistic 24-mode model Hamiltonian. *The Journal of Chemical Physics*, 110(2):936, 1999.

[42] Iakov Polyak, Charlotte SM Allan, and Graham A Worth. A complete description of tunnelling using direct quantum dynamics simulation: Salicylaldimine proton transfer. *The Journal of chemical physics*, 143(8):084121, 2015.

[43] TJA Wolf, Thomas Scheby Kuhlman, Oliver Schalk, TJ Martinez, Klaus Braagaard Møller, A Stolow, and A-N Unterreiner. Hexamethylcyclopentadiene: time-resolved photoelectron spectroscopy and ab initio multiple spawning simulations. *Physical Chemistry Chemical Physics*, 16(23):11770–11779, 2014.

[44] TJA Wolf, DM Sanchez, J Yang, RM Parrish, JPF Nunes, M Centurion, R Coffee, JP Cryan, M Gühr, K Hegazy, et al. The photochemical ring-opening of 1, 3-cyclohexadiene imaged by ultrafast electron diffraction. *Nature chemistry*, page 1, 2019.

[45] Hanneli R Hudock, Benjamin G Levine, Alexis L Thompson, Helmut Satzger, D Townsend, N Gador, S Ullrich, Albert Stolow, and Todd J Martinez. Ab initio molecular dynamics and time-resolved photoelectron spectroscopy of electronically excited uracil and thymine. *The Journal of Physical Chemistry A*, 111(34):8500–8508, 2007.

[46] T Northey, J Duffield, and TJ Penfold. Non-equilibrium x-ray spectroscopy using direct quantum dynamics. *The Journal of chemical physics*, 149(12):124107, 2018.